

Research Article

Ginsenoside CK Inhibits the Proliferation of Small Cell Lung Cancer Cells and Induces G2/M Cell Cycle Arrest and Apoptosis via the ATM/ATR Signaling Pathway

 **Paison Faida**,^{1,2,4}  **Jing Zhao**,^{1,2}  **Linlin Qu**,^{1,2}  **Ying He**,³  **Janvier Habumugisha**,⁵  **Xiaoxuan Ma**,^{1,2}
 **Rong Huang**,³  **Daidi Fan**,^{1,2}

¹Shaanxi Key Laboratory of Degradable Biomedical Materials and Shaanxi R&D Center of Biomaterials and Fermentation Engineering, Faculty of Chemical Engineering, Northwest University, Shaanxi, China

²Biotechnology & Biomedical Research Institute, Northwest University, Shaanxi, China

³Shaanxi Giant Biotechnology Ltd, Xi'an, Shaanxi, China

⁴Faculty of Education, Kigali Independent University, Kigali, Rwanda

⁵Department of Orthodontics, Faculty of Medicine, Dentistry and Pharmaceutical Sciences, Okayama University, Okayama, Japan

Abstract

Objectives: To explore the anti-tumor effect of Ginsenoside compound K (CK) on small cell lung cancer (SCLC). To elucidate the underlying mechanisms of CK's effects on SCLC.

Methods: Investigation through MTT, cell colony formation assays, and AO/EB staining to assess CK's effect on cell proliferation. Propidium iodide (PI), Annexin V/PI staining, TUNEL assay, and western blotting to analyze CK-induced DNA damage, G2/M arrest, and apoptosis in SCLC cells. A xenograft nude mice model to evaluate the in vivo effect of CK on tumor growth.

Results: CK effectively inhibits the proliferation of SCLC cells in vitro. CK induces DNA damage, G2/M cell cycle arrest, and apoptosis in SCLC cells in a dose-dependent manner. The anti-tumor effects of CK are mediated primarily through the ATM/ATR signaling pathway. In a xenograft model, CK treatment significantly inhibits tumor growth without causing notable side effects.

Conclusion: This study provides the first evidence of CK's anti-cancer efficacy in SCLC. The findings suggest that CK could be a promising therapeutic approach for SCLC, opening up new opportunities for ginsenosides in lung cancer treatment.

Keywords: Anti-cancer effect, apoptosis, ATM/ATR, ginsenoside compound K (CK), small cell lung cancer, xenograft model

Cite This Article: Faida P, Zhao J, Qu L, He Y, Habumugisha J, Ma X, et al. Ginsenoside CK Inhibits the Proliferation of Small Cell Lung Cancer Cells and Induces G2/M Cell Cycle Arrest and Apoptosis via the ATM/ATR Signaling Pathway. EJMO 2024;8(4):471–487.

Lung cancer holds a dominant position as the most prevalent form of cancer and carries the highest mortality rate among all cancer types globally.^[1] Small cell lung cancer (SCLC) and non-small cell lung cancer (NSCLC)

represent the two primary histological classifications of lung cancer. SCLC, known for its high aggressiveness, constitutes approximately 15% of all lung malignancies.^[2] SCLC is a formidable and life-threatening disease charac-

Address for correspondence: Paison Faida; Daidi Fan, MD. Shaanxi Key Laboratory of Degradable Biomedical Materials and Shaanxi R&D Center of Biomaterials and Fermentation Engineering, Faculty of Chemical Engineering, Northwest University, Shaanxi, China; Biotechnology & Biomedical Research Institute, Northwest University, Shaanxi, China

Phone: +86-29-88305118 **E-mail:** faidapaision@ul.ac.rw; fandaiddi@nwu.edu.cn

Submitted Date: September 11, 2024 **Accepted Date:** October 23, 2024 **Available Online Date:** December 09, 2024

©Copyright 2024 by Eurasian Journal of Medicine and Oncology - Available online at www.ejmo.org

OPEN ACCESS This work is licensed under a Creative Commons Attribution-NonCommercial 4.0 International License.



terized by a dismal prognosis. Its aggressive nature is attributed to rapid growth, a propensity for metastasis, and an abundance of cancer stem cells.^[3] In a clinical context, SCLC demonstrates swift growth and a heightened propensity for spreading to distant body regions. To address the elevated fatality associated with it, numerous scientists have concentrated on strategies to prevent lung cancer alongside initiatives for early detection and enhanced therapeutic approaches. Over the last few decades, there has been a gradual enhancement in the survival rate of NSCLC. In contrast, the survival rate of SCLC has exhibited minimal alteration over time.^[4,5] Indeed, when compared to the overall five-year survival rate for all types of lung cancer, the five-year survival rate for SCLC is notably low.^[6] An urgent demand is for new and efficient anti-cancer medications that improve clinical results while causing fewer and milder side effects.^[7]

SCLC treatment strategies include surgery, chemotherapy, and thoracic irradiation.^[8] Starting from the 1980s, the standard initial treatment for SCLC has involved chemotherapy using etoposide in combination with a single platinum-based agent.^[9] Initially, SCLC is susceptible to chemotherapy, but it swiftly acquires resistance to drugs as the tumor spreads.^[10] As outlined by the guidelines of the American Cancer Society, chemotherapy stands as the primary approach for treating SCLC, with cisplatin, etoposide, carboplatin, and irinotecan being the commonly employed medications. Nevertheless, these drugs demonstrate restricted effectiveness and produce substantial side effects.^[11] Medicinal herbs derived from natural products have captured considerable interest due to their exceptional effectiveness and minimal toxicity in the progression of cancer drug development.^[12] The primary bioactive component of ginseng, known as ginsenoside, has been scientifically demonstrated to exhibit remarkable pharmacological properties, including its effectiveness in combating tumors.^[13] Over the years, a range of effects attributable to CK has been documented, with particular emphasis on its potential as an anti-cancer agent. CK has garnered significant attention in cancer research and treatment owing to its potent anti-cancer properties. It has demonstrated the ability to inhibit cell proliferation, induce cell cycle arrest, and trigger apoptosis and autophagy in human cancer cells.^[14–17] However, the effect of ginsenoside CK on SCLC was not studied.

Many anti-cancer drugs exert their effects by halting the cell cycle and promoting apoptosis in cancer cells. The processes of inducing cell cycle arrest, facilitating DNA damage repair, and triggering apoptosis are substantially influenced by the activities of ataxia telangiectasia mutated (ATM) and ataxia telangiectasia and Rad3-related

(ATR), both of which play crucial roles in preserving genome integrity.^[18] When DNA damage is detected, certain sites on ATM and ATR are phosphorylated, activating them.^[19] The initiation of ATM and ATR activation leads to the consequent phosphorylation of downstream proteins like p53, checkpoint kinase 1 (CHK1), and CHK2. When p53 is phosphorylated at Ser15 by ATM or ATR, it hinders the binding of mouse double minute 2 homolog (Mdm2), resulting in the buildup of p53 and an enhanced capacity for its transcriptional activation [20]. ATM and ATR activate CHK1 and CHK2 in reaction to DNA damage or replication stress. These activated CHK1 and CHK2 play a crucial role in regulating the cell division cycle 25 (CDC25) phosphatase family, particularly CDC25A, CDC25B, and CDC25C. Through ATM/ATR pathways triggered by DNA damage or replication stress, CHK1 and CHK2 activation lead to the deactivation of CDC25s. This prompts cyclin-dependent kinases (CDKs) inhibition and induces cell cycle arrest.^[21,22] However, the impact of ginsenoside CK on prompting cell cycle arrest and apoptosis through the ATM/ATR signaling pathway in human small-cell lung cancer has not been investigated. This research endeavors to explore the anti-cancer potential of ginsenoside CK on SCLC and delves into its prospective molecular targeting mechanism by examining SCLC cell lines. Additionally, the study aims to assess the anti-tumor efficacy within a tumor xenograft model.

Methods

Materials and Chemicals

The study employed various chemicals and materials sourced from different providers. Ginsenoside CK was obtained from Chengdu Biopurify Phytochemicals Ltd. in Sichuan, China. Gefitinib was acquired from AstraZeneca in Cheshire, UK. Roswell Park Memorial Institute (RPMI-1640) cell culture media and penicillin/streptomycin were procured from HyClone in LA, USA. Fetal bovine serum (FBS) was sourced from GIBCO in NY, USA. Giemsa staining solution was purchased from Heart Biological Technology in Xi'an, China. The Pan-caspase inhibitor and Hoechst 33342 fluorescent dye were obtained from the Beyotime Institute of Biotechnology in Shanghai, China. All antibodies used in the study were purchased from Proteintech Group, Inc. Polyethylene glycol (PEG-400) was obtained from Longyuan Chemical in Zhengzhou, China. Dimethyl sulfoxide (DMSO) and methyl thiazolyl diphenyl tetrazolium bromide (MTT) were acquired from Aladdin Biotechnology in Shanghai, China. A cell cycle analysis kit was sourced from KeyGen Biotech in Nanjing, China.

Cell Culture

All H1688 and DMS114 cell recovery, medium replacement, passage, and cryopreservation were carried out according to the literature.^[23] Cell culture was placed in a 37 °C, 5% CO₂ incubator.

Cell Viability Assay

In this study, the MTT method was engaged to assess the inhibitory impact of ginsenoside CK on H1688 and DMS114 small-cell lung cancer cells. Two distinct types of small cell lung cancer cells, characterized by robust growth and a cell density exceeding 85%, were selected for experimentation. After washing with pre-cooled PBS, they are digested with 0.25% trypsin. After the digestion is completed, collect and centrifuge the cells. After centrifugation, use cell culture medium. After dilution and counting on a counting plate, dilute the cell density to 5×10⁴ cells/mL and inoculate it into a 96-well plate with 100 microliters per well. After incubating for 8 hours in a carbon dioxide cell incubator, discard the culture medium and use different concentrations of CK (0, 10, 20, 30, and 40 μM) for 24 and 48 h respectively. After 24 and 48 hours, 50 μL of MTT solution with a concentration of 1 mg/mL was added to each well and continued culturing in the incubator for 4 hours. Then aspirate the MTT solution, add 150 μL dimethyl sulfoxide to each well, shake on the shaker, detect the OD value at 490 nm with a microplate reader, and use the following formula to calculate the cell viability:

Cell survival rate (%) = (OD value of experimental group / OD value of control group) × 100%

Colony Formation Assay

H1688 and DMS114 cells were seeded and grown, then collected, washed with PBS, digested, centrifuged, counted, and then added to a 6-well plate (300 cells per well). After 24 h, ginsenoside CK (0, 10, 20, and 30 μM) was added and cultured for 24 h. Then use complete culture medium to continue culturing. After about two weeks, obvious colony formation can be observed. Then wash with PBS, add methanol to fix for 10 minutes, add Giemsa working solution for staining for 10 minutes after washing with PBS, and then wash with PBS. Observe under a microscope, take pictures, and record the number of colonies formed in each well. Ultimately, ImageJ software quantified the number of colonies containing 50 cells or more.

Detection of Cell Cycle Distribution

The impact of ginsenoside CK on the cycle distribution of two small cell lung cancer cell lines was examined using flow cytometry. H1688 and DMS114 cells were grown and digested with 0.25% trypsin respectively, collected and centrifuged, and after counting on a cell counting plate, diluted to 2×10⁵

cells/well, inoculated evenly in a 6-well plate, and waited until the cells were cultured for 8 hours and adhered, 0, 10, 20 and 30 μM ginsenoside CK solutions were added respectively, and the drug acted for 24 hours. Remove the supernatant, add trypsin, centrifuge and collect, wash with PBS, fix the cells in 75% ethanol at 4°C overnight, centrifuge to remove the supernatant, and then add the prepared PI/RNase A staining working solution. Stain at room temperature in the dark for 30-60 minutes, and finally use flow cytometry (Becton Dickinson, CA) to detect cell cycle distribution. The obtained data were then analyzed using FlowJo software.

Quantification of Apoptosis using Annexin V/PI Staining

H1688 and DMS114 cells were grown, digested with 0.25% trypsin, collected, and centrifuged, and after counting on a cell counting plate, dilute them to 2×10⁵ cells/well and place them in a 6-well plate. Inoculate evenly in the medium. After the cells have adhered to the culture for 8 hours, 0, 10, 20, and 30 μM ginsenoside CK solutions are added respectively, and the drug acts for 24 hours. Remove the supernatant, digest with trypsin, centrifuge and collect, wash twice with PBS, add Annexin V-FITC, mix well, and react in the dark for 5 to 15 minutes. Finally, use a flow cytometer to detect the cell apoptosis rate.

Hoechst 33342 Staining Assay

Hoechst 33342 staining was used to examine the cell morphology. In a 6-well plate, H1688 and DMS114 cells (2×10⁵ cells/mL) were cultivated. After being exposed to CK (0, 10, 20, 30 M) for 24 hours, H1688 and DMS114 cells were rinsed with PBS and then incubated with Hoechst 33342 (Solarbio, Beijing, China). UV illumination was used to observe the Cell morphological features through an inverted fluorescence microscope.

AO/EB Staining Assay

The morphological characteristics of apoptosis in small cell lung cancer cells under the influence of ginsenoside CK were observed using the AO/EB double staining method. Take H1688 and DMS114 cells, digest them with trypsin respectively, collect and centrifuge, and after counting on a cell counting plate, dilute them to 2×10⁵ cells/well, inoculate them evenly in a 6-well plate, and wait for culture for 8 hours. After the cells adhered for 1 hour, 0, 10, 20, and 30 μM ginsenoside CK solutions were added respectively, and the drug was allowed to act for 24 hours. Add pre-cooled PBS and wash twice, then add AO/EB mixture (AO 100 mg/mL and EB 100 mg/mL) for staining for 5-10 minutes, and observe and take pictures under an inverted fluorescence microscope (Nikon, Japan).

Western Blotting

In the conducted study, H1688 and DMS114 cells were cultured in a 6-well plate at a concentration of 5×10^5 cells/mL and exposed to varying concentrations of CK (0, 10, 20, 30 μ M) for a duration of 24 hours. Subsequent to the treatment, the cell samples underwent two washes with PBS and were lysed on ice in RIPA buffer (Beyotime, Shanghai, China), supplemented with 1% PMSF, 1% phosphorylated inhibitors (Solarbio, Beijing, China), and 1 mM phenylmethylsulfonyl fluoride (PMSF) for 35 minutes. Following lysis, the cell lysates were centrifuged at 12,000 rpm for 25 minutes at 4 °C, and the protein concentrations were quantified using the BCA Assay kit (Thermo Fisher, Shanghai, China). The separated proteins were then subjected to SDS-PAGE and electro-transferred onto polyvinylidene fluoride (PVDF) membranes. These membranes were subsequently blocked with 5% nonfat milk in TBST for 2 hours at room temperature, followed by overnight incubation with the respective primary antibodies at 4°C. Afterward, the membranes underwent five washes with $1 \times$ TBST and were exposed to HRP-conjugated secondary antibodies for 1 hour at room temperature. The protein bands were visualized using an ECL system (Tanon, Shanghai, China).

Human Lung Cancer Xenograft Nude Mouse Model

To investigate the potential tumor-suppressing effects of ginsenoside CK on small cell lung cancer (SCLC), we established a model using nude mice bearing tumors. Female nude mice were obtained and raised in conditions that are free from specific pathogens (SPF). After a week of getting accustomed to the environment, the mice were injected with H1688 cells at a cell density of 1×10^7 cells/cell. Before injection, the skin of the nude mice was locally disinfected, and the inoculation was done through subcutaneous injection into the left armpit. Once the tumor volume reached 100-150 mm³, mice with similar tumor sizes were chosen and divided into four groups (n=5): (1) Control group: receiving daily intraperitoneal injections of a mixture of 5% Tween 80 and 95% saline; (2) Low-dose ginsenoside CK group: receiving daily intraperitoneal injections of 25 mg/kg ginsenoside CK; (3) High-dose ginsenoside CK group: receiving daily intraperitoneal injections of 50 mg/kg ginsenoside CK; (4) Cisplatin positive control group: receiving intraperitoneal injections of 4 mg/kg cisplatin every three days. Throughout the experimental duration, the body weight and tumor size of the nude mice were regularly monitored every two days. The tumor volume was calculated using the formula: $V = 0.5 \times \text{long diameter of the tumor} \times \text{short diameter of the tumor} \times \text{short diameter of the tumor}$ (mm³). After 21 days of treatment, the nude mice were euthanized humanely.

Tumor blocks were then extracted and preserved either in liquid nitrogen or fixed in formalin/2.5% glutaraldehyde for subsequent analyses, including western blot analysis, H&E staining, immunohistochemistry analysis, and transmission electron microscopy analysis. Additionally, the primary organs (heart, liver, spleen, lungs, and kidneys) of nude mice from different experimental groups were harvested, fixed in formalin, and subjected to H&E staining analysis.

Hemogram Assay and Measurement of Biochemical Parameters

On the 21st day of the investigation, blood and serum samples were obtained from each experimental group. Peripheral blood was drawn from the orbital venous plexus and placed in tubes containing ethylenediaminetetraacetic acid (EDTA) for the assessment of hematological parameters, including the white blood cell (WBC) count, lymphocyte (LYM) count, and granulocyte (GRAN) count. This analysis was conducted using an automated hematology analyzer (HC2200, Meiyilinm, China). Additionally, on the 21st day, serum samples were collected and used to examine liver function indicators, including alanine aminotransferase (ALT) and aspartate transaminase (AST). Furthermore, renal function parameters such as urea, uric acid (UA), and creatinine were scrutinized using commercial kits following the guidelines provided by the manufacturer (Shanghai Enzyme Biotechnology Co., Ltd, Shanghai, China).

Histopathology and Immunohistochemistry

We embedded tumor tissues, as well as vital organs such as the heart, liver, spleen, lungs, and kidneys, in paraffin. Subsequently, 5 μ m sections were prepared and subjected to hematoxylin and eosin (H&E) staining. The assessment of Ki67 expression in the tumor tissues was conducted using an immunohistochemistry assay, and the resulting images were captured using a microscope.

TUNEL Assay

The TUNEL assay was utilized to identify apoptosis within tumor tissues. In a concise description, the tissues were first fixed in a 4% paraformaldehyde solution for a period ranging from 4 to 24 hours at a temperature of 4°C. Following fixation, the tissues were cryosectioned into thin 5 μ m slices, subsequently undergoing permeabilization with 0.2% Triton X-100. This was followed by incubation with a TUNEL reaction mixture that contained both nucleotide mixture and terminal deoxynucleotidyl transferase (TdT), which was carried out for 1 hour at 37°C. The stained cells were then subjected to PBS washing and observed utilizing a fluorescence microscope manufactured (Nikon, Japan).

Statistical Analysis

The statistical analysis was carried out using either the GraphPad Prism 8.0.1 software package or SPSS 19.0 software (SPSS Inc., USA). The findings were expressed as means±standard deviation (SD) derived from three or more independent samples. A P-value below 0.05 was deemed statistically significant.

Results

Inhibitory Effect of Ginsenoside CK on the Proliferation of SCLC Cells

To investigate the inhibitory effect of ginsenoside CK on SCLC cells, two distinct small-cell lung cancer cell lines, H1688 and DMS114 cells were subjected to varying concentrations of ginsenoside CK for 24 and 48 hours, and cell viability was judged using the MTT assay. The experimental findings reveal that with increasing exposure time and dosage of ginsenoside CK, its inhibitory effect on both SCLC cell lines intensifies, demonstrating a concentration- and time-dependent relationship. In comparison to the control group, these effects are statistically significant (* $p < 0.05$ or ** $p < 0.01$, Fig. 1A, B). Moreover, AO/EB double staining was performed to confirm the effects of ginsenoside CK on H1688 and DMS114 cell viability. AO/EB staining assay revealed that the number of cells that displayed red-orange fluorescence was concentration-dependently greater in both treated H1688 and DMS114 cells (Fig. 1C). Furthermore, colony formation experimental results are shown in Fig. 1D. As the dose of ginsenoside CK increases, the number of cell colonies formed by H1688 and DMS114 cells gradually decreases.

Effect of Ginsenoside CK on Cycle Distribution of H1688 and DMS114 Cells

The effect of ginsenoside CK on the cell cycle distribution of H1688 and DMS114 cells was evaluated using flow cytometry, and the outcomes are depicted in Figure 2A. In comparison to the control group, exposure to 30 μM ginsenoside CK resulted in an increased proportion of G2/M phase cells in both H1688 and DMS114 cells, along with a decrease in G1 and S phase cells. Moreover, to explore the molecular mechanisms driving SCLC cell cycle arrest induced by ginsenoside CK, Western blotting was employed to assess the expression of proteins associated with the G2/M cell cycle. As presented in Figure 2B, the results indicated a significant elevation in the expression levels of cyclin B1 protein, phosphorylated cdc2 protein, phosphorylated cdc25c protein, and p21 protein in both H1688 and DMS114 cells with escalating concentrations of ginsenoside CK. Simultaneously, the expression levels of cdc2 protein demonstrated

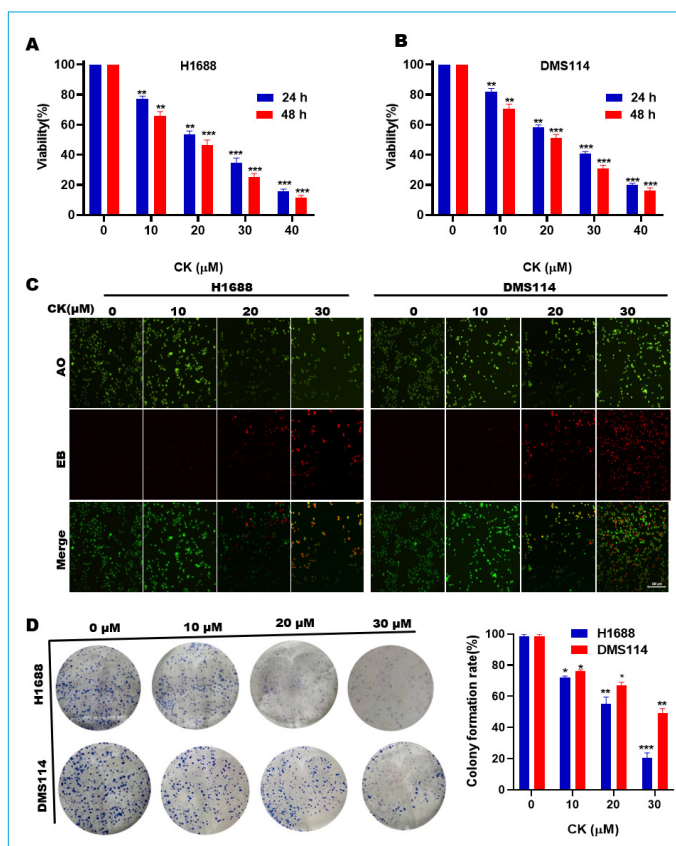


Figure 1. Ginsenoside CK inhibited the proliferation of SCLC cells in vitro. (a) The cell viability of H1688 and (b) DMS114 cells. (c) AO/EB staining via fluorescence microscopy. (d) The colony formation of H1688 and DMS114 cells. Data are presented as the means±SD of triplicate experiments, * $p < 0.05$, ** $p < 0.01$, *** $p < 0.001$ compared with the control.

a noticeable concentration-dependent reduction. These changes are statistically significant compared to the blank control group (* $p < 0.05$ or ** $p < 0.01$). These data confirmed that ginsenoside CK induces G2/M phase arrest in small cell lung cancer cells by influencing crucial cell cycle-related proteins in a concentration-dependent manner.

CK-Induces Caspase-Dependent Apoptosis in SCLC Cells

To investigate whether the inhibitory effect of ginsenoside CK on small-cell lung cancer cells is attributed to apoptosis, Hoechst 33342 fluorescent staining was engaged to observe morphological changes in H1688 and DMS114 cells following ginsenoside CK treatment. Hoechst 33342 staining solution, with slight cell permeability, revealed distinct morphological alterations. As depicted in Figure 3A, the control group displayed light blue, uniformly stained, and intact nuclei. Conversely, post-treatment with ginsenoside CK resulted in a significant reduction in cell numbers, displaying a dose-dependent effect. Moreover, for a quanti-

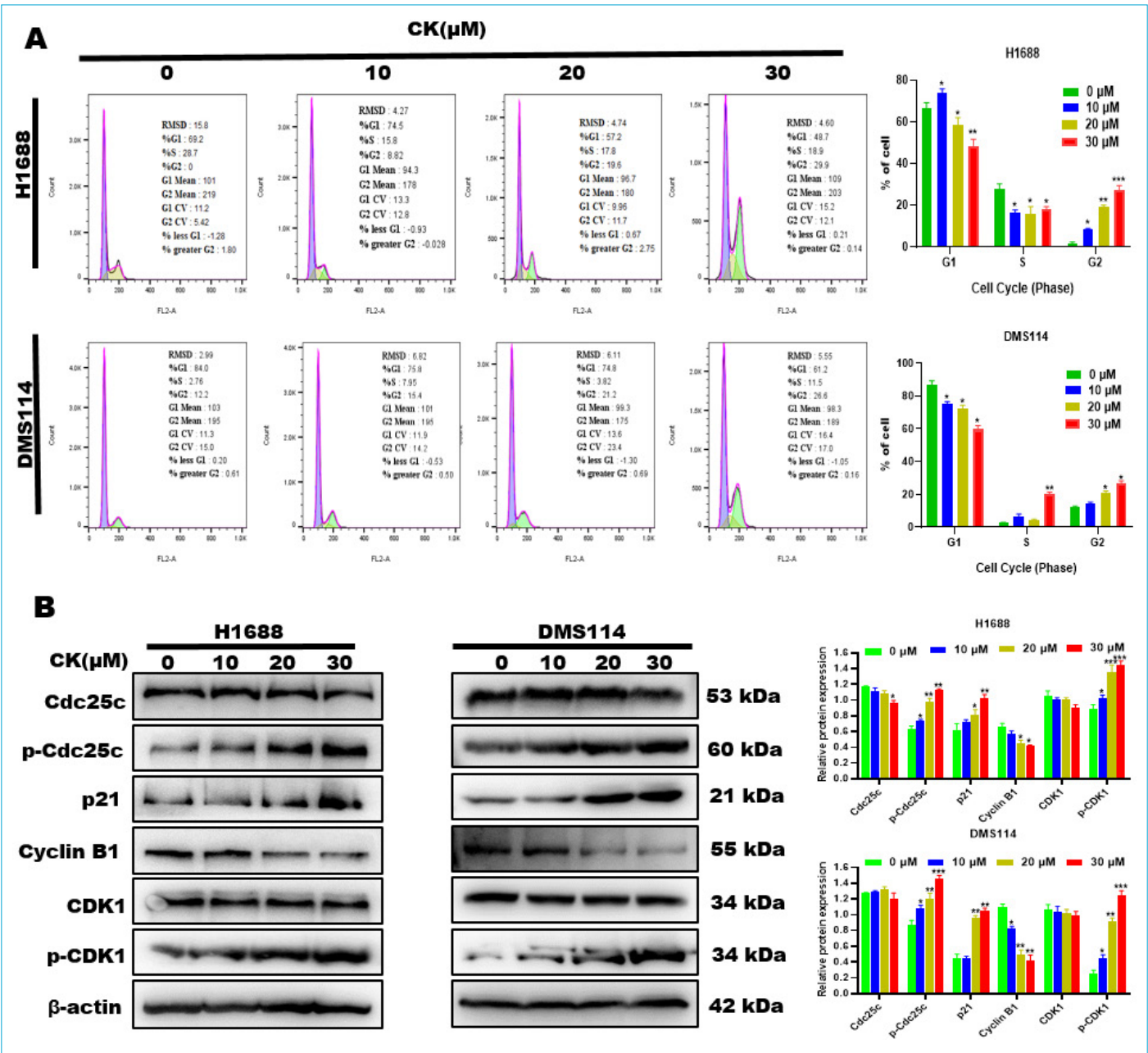


Figure 2. (a) Effect of ginsenoside CK on the cell cycle distribution in SCLC cells. **(b)** Expression levels of G2/M cell cycle-related proteins in SCLC cells following ginsenoside CK treatment. The data are depicted as means±SD of triplicate experiments, *p<0.05, **p<0.01 in comparison to the control group.

tative analysis of SCLC cell apoptosis, flow cytometry Annexin V/PI double staining was conducted to assess the impact of ginsenoside CK on apoptosis. Annexin V, able to enter intact cell membranes, in combination with PI dye, which penetrates damaged cell membranes, allowed for the distinction of cells at various stages of apoptosis. As illustrated in Figure 3B, the number of early and late apoptotic cells in both H1688 and DMS114 cells markedly increased following ginsenoside CK treatment in a concentration-dependent manner, with all showing signifi-

cant differences (**p<0.01). Furthermore, TUNEL staining was employed to validate CK-induced apoptosis in tumor tissues. The control group exhibited few apoptotic H1688 cells, whereas the CK-treated and cisplatin-treated groups exhibited a dose-dependent increase in TUNEL-positive H1688 cells (Figure 3C). Additionally, to elucidate the molecular mechanism underlying the induction of apoptosis in small-cell lung cancer (SCLC) cells by ginsenoside CK, the protein expressions associated with cell apoptosis were examined through western blotting. As illustrated in Figure

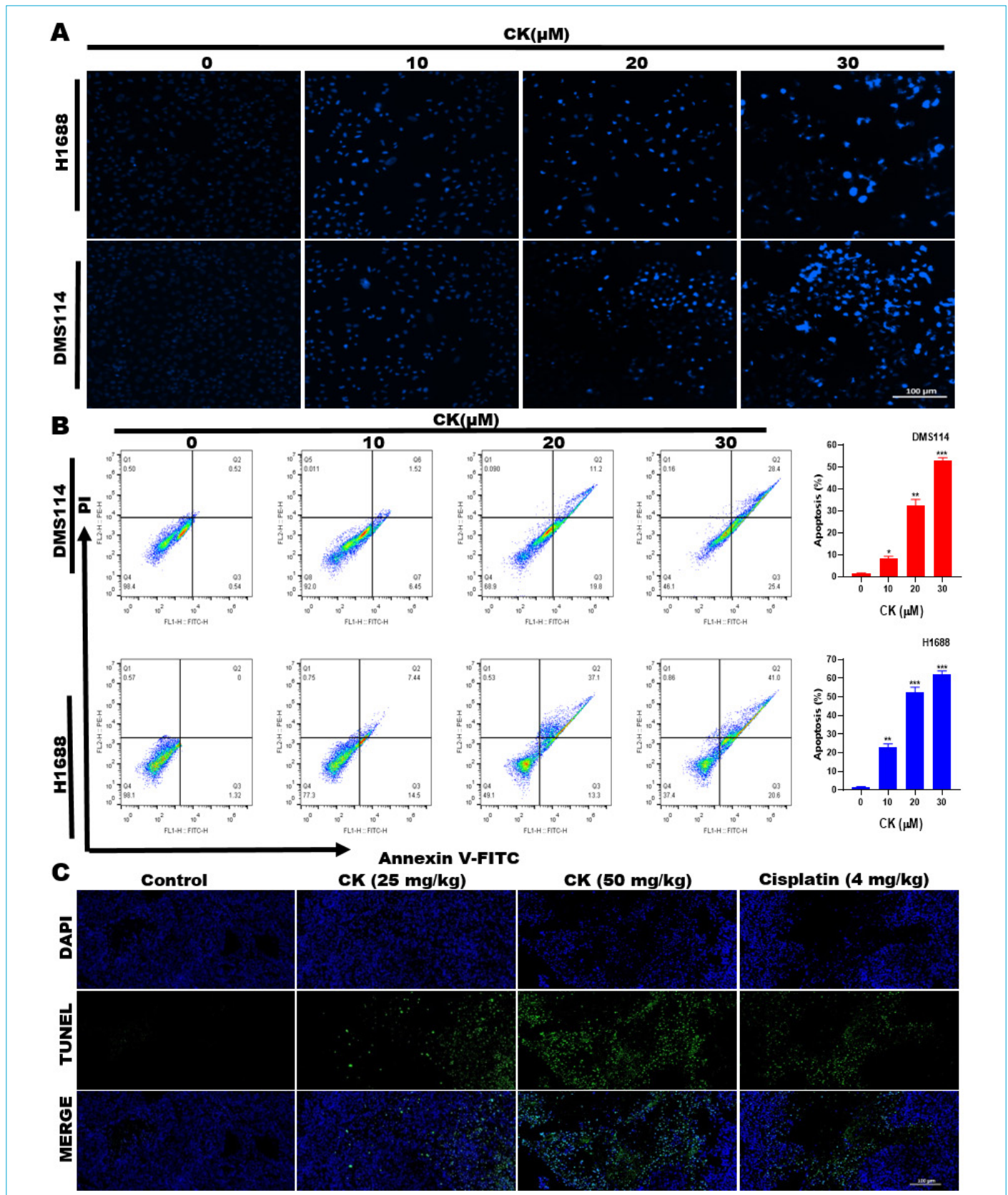


Figure 3. Ginsenoside CK-induced apoptosis of SCLC cells. **(a)** SCLC cells were stained with Hoechst 33342, Scale bar = 100 μ m. **(b)** Flow cytometry analysis was performed using Annexin V/PI staining **(c)** TUNEL staining of tumor tissues, Scale bar = 50 μ m. Values are expressed as mean \pm SD (n=3), *p<0.05, **p<0.01, ***p<0.001 compared with the control.

4A, the experimental results indicate that, with an increase in ginsenoside CK concentration, the expression levels of key members of the mitochondrial apoptosis pathway in SCLC cells p53 protein, Bax, cleaved caspase-9, cleaved caspase-3, and cleaved PARP were significantly upregulated. In contrast, the expression of Bcl-2 protein exhibited a notable dose-dependent decrease compared to the control group (* $p < 0.05$ or ** $p < 0.01$). To further validate the apoptotic effect of ginsenoside CK on SCLC cells, Z-VAD-FMK, a pan-caspase inhibitor capable of inhibiting caspase activity, was employed. H1688 and DMS114 cells were pre-treated with Z-VAD-FMK at a concentration of 60 μM for 2 hours, followed by treatment with ginsenoside CK at a concentration of 20 μM . MTT experiments demonstrated that Z-VAD-FMK mitigated the impact of CK on SCLC cell viability. In comparison to the ginsenoside CK group, after Z-VAD-FMK treatment, the viability of small cell lung cancer cells noticeably increased (## $p < 0.01$, Figure 4B, C). Finally, the study investigated the expression changes of apoptosis-related proteins in SCLC cells following Z-VAD-FMK treatment. Z-VAD-FMK significantly reduced the expression levels of cleaved caspase-3 and cleaved PARP proteins compared to those treated with CK alone (# $p < 0.05$, Figure 4D). These findings suggest that ginsenoside CK induces SCLC cell apoptosis by activating the mitochondrial apoptosis pathway.

CK Suppressed H1688 Tumor Growth in Vivo

Based on the results of in vitro experiments, H1688 cells were chosen as the central focus of the study, and a xenograft tumor model for human small-cell lung cancer (SCLC) was established to assess the suppressive effects of ginsenoside CK on SCLC in vivo. In the xenograft model using H1688 cells in nude mice bearing small-cell lung cancer, the in vivo inhibitory effect of ginsenoside CK on SCLC was investigated through subcutaneous administration. The morphological changes in the tumors after 21 days of administration are depicted in Figure 5A, indicating that both the ginsenoside CK groups and the cisplatin group significantly hindered the growth of small-cell lung cancer. Furthermore, Figure 5B demonstrates that, following 21 days of administration, the low-dose ginsenoside CK group, high-dose ginsenoside CK group, and cisplatin group substantially reduced the tumor weight by 47.02%, 76.24%, and 78.26%, respectively, compared to the negative control group. All treatment groups exhibited significant differences ($p < 0.05$), with the high-dose ginsenoside CK group achieving a nearly equivalent effect to the positive control cisplatin group. The impact of ginsenoside CK and cisplatin on the tumor volume of tumor-bearing nude mice is presented in Figure 5C. In comparison to the negative con-

trol group, the low-dose ginsenoside CK group, high-dose ginsenoside CK group, and cisplatin group demonstrated a slower increase in tumor volume. After 21 days of administration, the average tumor volume in the low-dose ginsenoside CK group was 857.79 mm^3 , and in the high-dose ginsenoside CK group, it was 386.68 mm^3 , both showing significant differences ($p < 0.05$) compared to the negative control group. The cisplatin-treated group had an average tumor volume of 308.75 mm^3 , also significantly different from the negative control group. Moreover, to explore the therapeutic impact of ginsenoside CK on H1688 small-cell lung cancer tumor-bearing nude mice, tumor tissues were extracted, and H&E staining was conducted to observe the influence of ginsenoside CK on tumor tissue. The H&E staining results in Figure 5E revealed that in H1688 small-cell lung cancer tumor-bearing nude mice, the control group exhibited a high number of tumor cells with deep staining, while the 50 mg/kg CK treated group displayed a decrease in tumor cells, with a low cell density. Additionally, there were significantly reduced areas of light-staining tumor tissue with numerous regions of necrosis and fibrosis, as observed in the H&E staining of tumor tissues from tumor-bearing nude mice. Moreover, the expression of Ki67, a molecular marker for cell proliferation, was assessed. As shown in Figure 5F, the Ki67 expression levels in the high-dose CK-treated and cisplatin-treated groups were significantly reduced compared to the control group. These findings suggest that ginsenoside CK significantly inhibits the growth of tumors in nude mice bearing small-cell lung cancer.

Toxicity Evaluation of CK in the Xenograft Nude Mice

After establishing the xenograft model using H1688 small cell lung cancer tumor-bearing nude mice, we investigated the impact of ginsenoside CK and cisplatin on the body weight of these mice (Fig. 5D). Throughout the 21-day administration period, both CK-treated mice and control mice consistently showed an increase in weight. However, the body weight of mice in the cisplatin-treated positive control group initially increased for the first 6 days and then began to decline, indicating the toxicity of cisplatin ($p < 0.05$). Moreover, we assessed whether ginsenoside CK and cisplatin influenced the normal function of immune cells in the peripheral blood of nude mice in various groups, including the normal group (normally fed nude mice without tumor inoculation), the negative control group, low-dose and high-dose ginsenoside CK groups, and the cisplatin group. According to the results, there was no significant difference in the counts of white blood cells (WBC), granulocytes (GRAN), and lymphocytes (LYM) in the peripheral blood between the normal group, normal + high dose CK

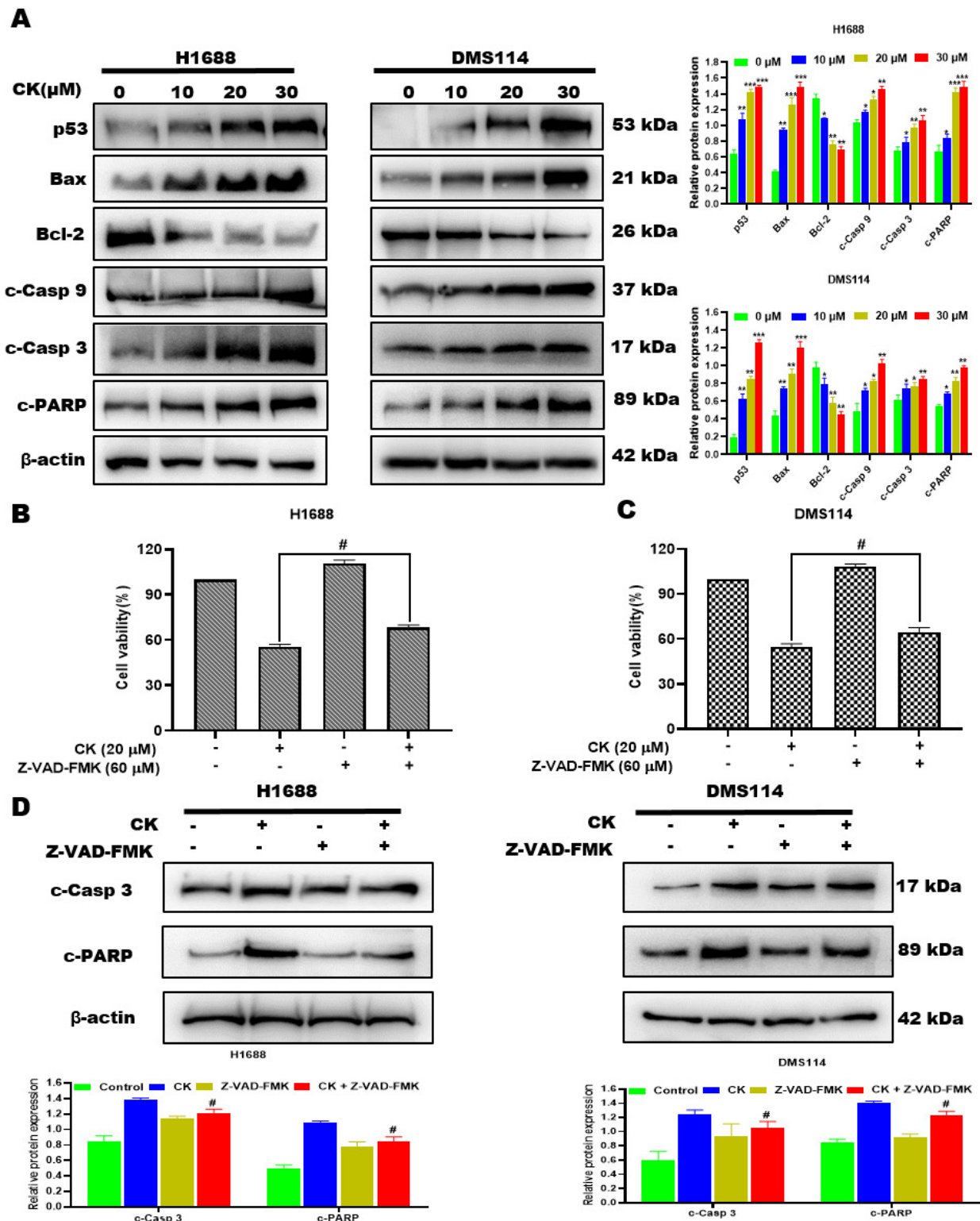


Figure 4. Ginsenoside CK triggers apoptosis via intrinsic pathways in human small-cell lung cancer cells. **(a)** The levels of apoptosis-related proteins in both H1688 and DMS114 cells were evaluated using western blotting. H1688 cells **(b)** and DMS114 cells **(c)** were pre-treated with 60 μ M Z-VAD-FMK for 2 hours, followed by simultaneous treatment with ginsenoside CK (50 μ M) for an additional 24 hours. Subsequently, cells were subjected to the MTT assay. **(d)** Cells were pre-treated with 60 μ M Z-VAD-FMK for 2 h, followed by co-treatment with ginsenoside CK (50 μ M) for an additional 24 h, and the expression of apoptosis-related proteins was then examined using western blotting. * $p < 0.05$; ** $p < 0.01$ compared to the control; # $p < 0.05$; ## $p < 0.01$ compared to control cells treated with ginsenoside CK.

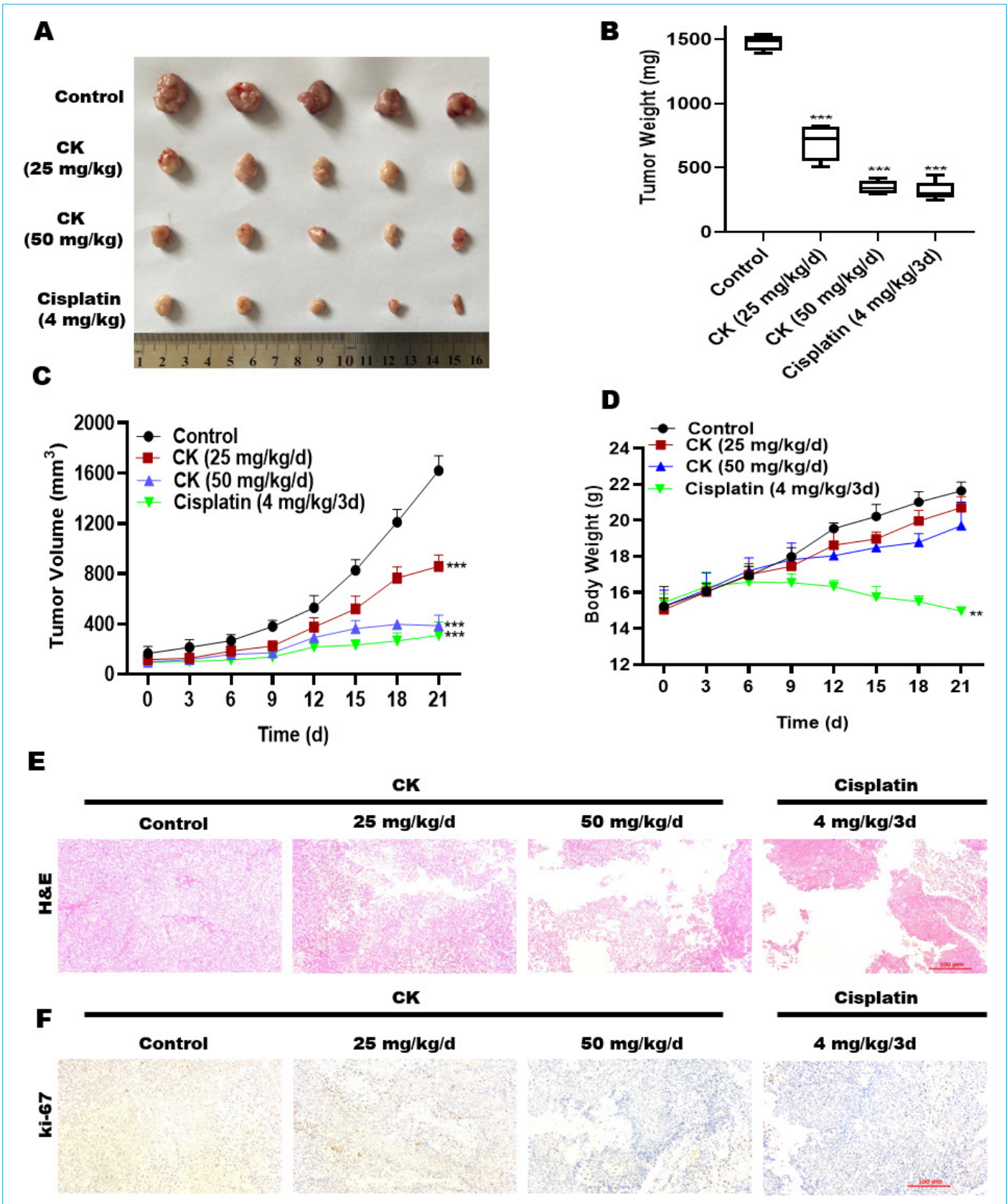


Figure 5. Ginsenoside CK significantly inhibited the proliferation of tumors in H1688 subcutaneous tumor-bearing mice. (a) Representative image of H1688-xenograft tumor. (b) Tumor weight. (c) Tumor volume. (d) Body weight. (e) H&E staining of tumor tissue. (f) Immunohistochemistry assays. All data are presented as the means±SD of triplicate experiments, *p<0.05, **p<0.01, ***p<0.001 compared with the control.

group, control group, low dose CK group, and high dose CK group. However, the counts of these immune cells in the cisplatin group were reduced compared to those in the normal group (Fig. 6A), suggesting that cisplatin might compromise the immune system of the nude mice, while CK did not exhibit such immune-suppressive effects. Moreover, we examined the impact of CK on hepatic and renal functions. After administering CK to mice for 21 days, there were no significant alterations in liver function parameters, namely alanine aminotransferase (ALT) and aspartate transaminase (AST), or renal function parameters (blood urea nitrogen and creatinine) when compared to the control group. Thus, CK did not negatively affect the liver or kidneys. Conversely, the liver function parameters of cisplatin-treated mice were notably elevated, indicating that cisplatin had adverse effects on liver function ($p < 0.05$, Fig. 6B, C). Furthermore, the vital organs (heart, liver, spleen, lungs, and kidneys) of nude mice with small-cell lung cancer in different groups were removed for H&E staining analysis, aiming to observe the effects of ginsenoside CK and cisplatin on the internal organs of tumor-bearing nude mice. As depicted in Figure 6D, the heart, liver, spleen, lungs, and kidneys of the normal group, negative control group, and ginsenoside CK-treated groups exhibited no signs of damage. In contrast, cisplatin demonstrated damaging effects on the spleen, liver, and kidneys of nude mice. In conclusion, these findings affirm that CK does not have adverse effects on the normal functions of vital organs and immune cells *in vivo*.

Ginsenoside CK Induced Changes in the DNA Damage Response and Activated the ATM/ATR Signaling Pathway in SCLC Cells

Cell cycle arrest commonly arises from DNA damage, and a swift response to induce double-strand breaks in DNA involves the phosphorylation of the histone variant H2AX at Ser-139, known as γ -H2AX. This phosphorylation results in the formation of distinct DNA damage-induced nuclear foci. To evaluate whether ginsenoside CK induces DNA damage, we examined the phosphorylation of γ -H2AX through western blot analysis. In both H1688 and DMS114 cells treated with ginsenoside CK, we observed a notable increase in phosphorylated H2AX in a dose-dependent manner (Fig. 7A). Previous research has also indicated that the accumulation of functional p53 plays a pivotal role in the apoptosis process induced by chemotherapy.^[24] Western blot analysis conducted in this study demonstrated a dose-dependent elevation in p53 protein expression 24 hours after treatment with ginsenoside CK. It is noteworthy that DNA damage-sensing kinases such as ATM, ATR, and checkpoint kinases (Chk1 and Chk2) are known to regulate

the p53 protein.^[25,26] The ATM/ATR pathway plays an important role in DNA homologous recombination repair.^[27] The effect of ginsenoside CK on the ATM/ATR-CHK2/CHK1 Signaling Pathway was also investigated in this study. Because two distinct kinase signaling cascades, the ATM-CHK2 and ATR-CHK1 pathways, coordinate cellular responses to DNA damage,^[28] This study used western blot analysis to assess the expression levels and phosphorylation states of ATM (Ser1981), ATR (Ser428), CHK2 (Thr68), and CHK1 (Ser345) in H1688 and DMS114 cells treated with ginsenoside CK. This analysis aimed to determine whether ginsenoside CK treatment activates DNA damage-sensing kinases in these cells. As portrayed in Figure 7A, while the overall protein levels of ATM, ATR, CHK2, and CHK1 remained constant, their phosphorylation levels exhibited a significant increase. To further confirm the involvement of the ATM/ATR pathway in SCLC, experiments were conducted using the ATM/ATR inhibitor, caffeine. H1688 and DMS114 cells treated with ginsenoside CK, in the absence or presence of caffeine, demonstrated that the ATM/ATR inhibitor effectively impeded the activation of the ATM/ATR-CHK2/CHK1 signaling pathway induced by ginsenoside CK. Caffeine, an inhibitor of the ATR/ATM signaling pathway, was used at a concentration of 10 mM to pretreat H1688 and DMS114 cells for 2 hours, followed by treatment with CK (20 μ M) for 24 hours. The MTT experiment results indicated that pretreatment of small cell lung cancer cells with caffeine could reverse the cell death induced by ginsenoside CK. After pretreatment with caffeine, the survival rates of H1688 cells treated with 20 μ M ginsenoside CK increased from 55.3% to 68.3%, compared to those treated with ginsenoside CK alone, showing a significant difference ($\#p < 0.05$; Fig. 7B). Similarly, after pretreatment with caffeine, the survival rates of DMS114 cells treated with 20 μ M ginsenoside CK increased from 56.7% to 69.7%, compared to those treated with ginsenoside CK alone, also displaying a significant difference ($\#p < 0.05$; Fig. 7C). The western blot experiments illustrated in Figure 7D demonstrated that caffeine induced the phosphorylation of ATM/ATR downstream proteins, while maintaining the overall protein levels of ATM, ATR, CHK2, and CHK1 constant. Notably, their phosphorylation levels exhibited a significant increase. These findings strongly suggest that ginsenoside CK activates DNA damage-sensing kinases.

Discussion

Small cell lung cancer (SCLC) is characterized by high aggressiveness and resistance to chemotherapy, making it one of the most challenging malignant tumors to treat. Additionally, the side effects associated with chemotherapy often impose limitations on the successful treatment

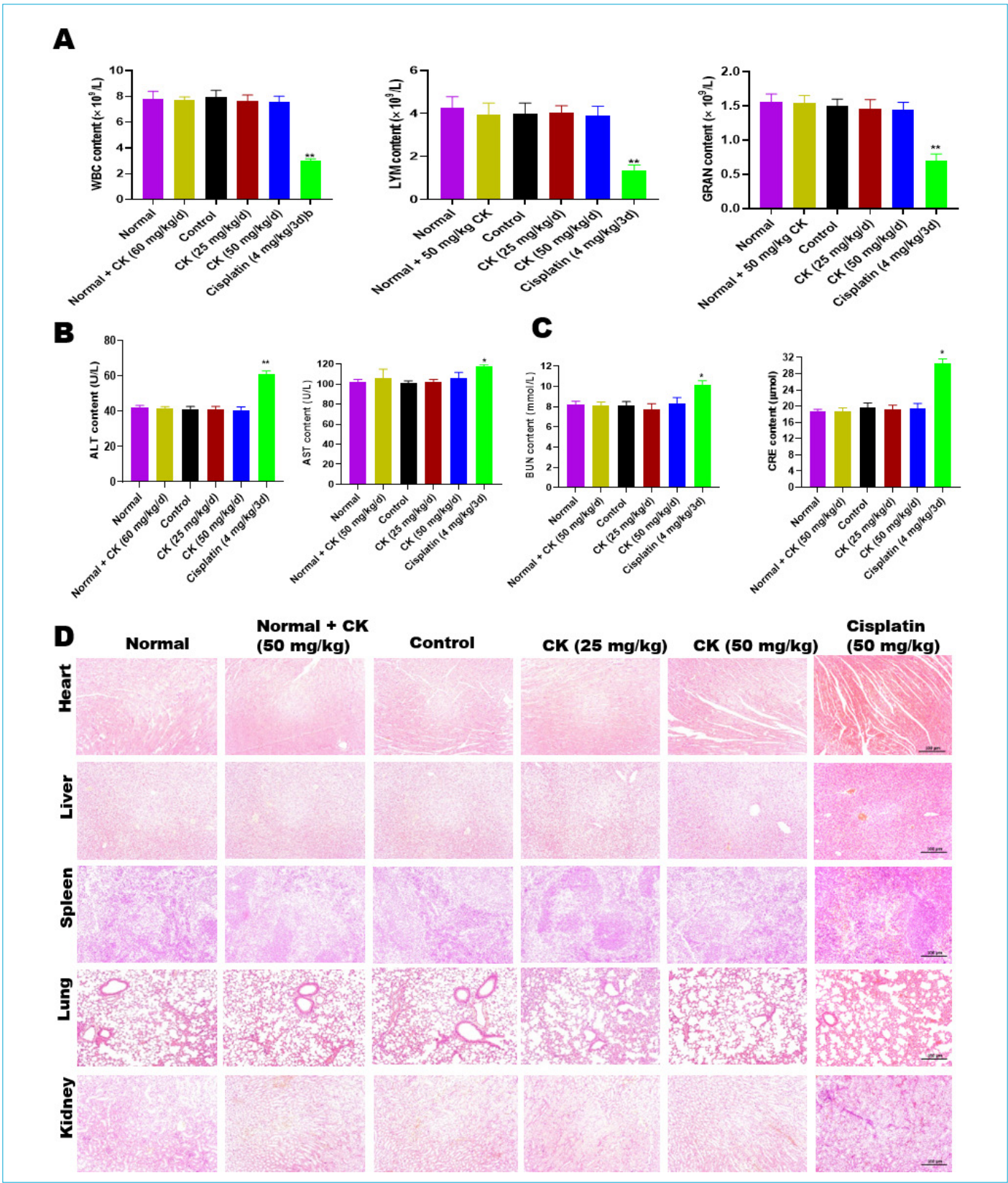


Figure 6. Effect of ginsenoside CK on major organs. **(a)** Enumeration of white blood cells (WBC), lymphocytes (LYM), and granulocytes (GRAN) in the peripheral blood of each experimental group. **(b)** Serum levels of liver function parameters (ALT and AST) across all groups. **(c)** Evaluation of renal function parameters (BUN and CRE). **(d)** H&E staining of vital organs. The data are represented as means \pm SD of triplicate experiments, * p <0.05, ** p <0.01, *** p <0.001 in comparison to the control. Scale bar = 100 μ m.

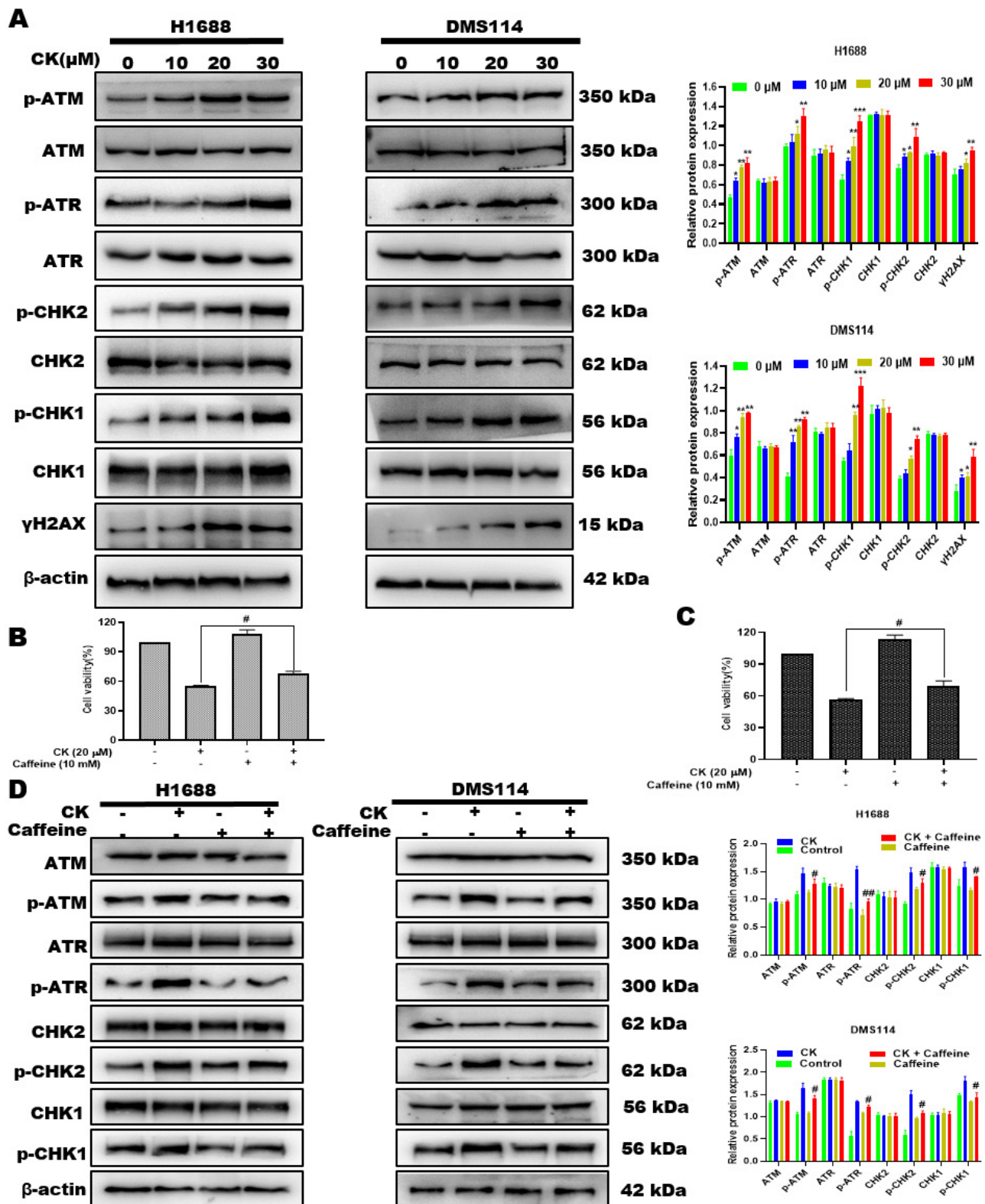


Figure 7. Effect of ginsenoside CK on the ATM/ATR-CHK1/CHK2 signaling pathway in small cell lung cancer cells. **(a)** Western blotting was performed to analyze the protein expression levels in SCLC cells after 24 h of CK treatment. **(b)** H1688 cell viability and **(c)** DMS114 cell viability were determined by MTT. **(d)** H1688 and DMS114 cells were treated with CK (50 μ M) with and without Caffeine (10 mM), and proteins were determined by western blotting. β -actin was used as an endogenous reference. All data are presented as means \pm SD from at least three independent experiments. * p <0.05, ** p <0.01, compared with control, # p <0.05, ## p <0.01, compared with the CK-treated group.

of lung cancer.^[29,30] Hence, there is a pressing demand for novel therapeutic approaches, and ginsenoside CK has exhibited potent anti-cancer properties against diverse types of tumors. In-depth mechanistic investigations have consistently shown that CK hinders cancer cell proliferation by inducing cell cycle arrest, fostering apoptosis, suppressing angiogenesis, and enhancing the sensitivity of colon cancer and neuroblastoma cells.^[31–33] However, there is currently no available information regarding the inhibitory actions of ginsenoside CK on small cell lung cancer (SCLC). This investigation was undertaken to explore the anti-proliferative effects and underlying molecular mechanisms of CK in both in vitro and in vivo settings. Our findings unveiled the anti-tumor efficacy of CK against SCLC, operating through apoptotic and cell cycle arrest pathways. The results indicated that CK impeded the growth of H1688 and DMS 114 cells following a 24-hour incubation period. In vitro experiments, including MTT, colony formation, and AO/EB staining, affirmed the effective suppression of proliferation in H1688 and DMS 114 cells by CK. Moreover, in a xenograft model involving nude mice, CK demonstrated inhibitory effects on tumor growth. Notably, CK significantly diminished the expression of Ki-67 in tumor tissues, indicating its inhibitory influence on tumors. Crucially, H&E staining disclosed that both the low-dose and high-dose CK groups did not adversely impact the normal functions of vital organs. Serum biochemical parameter assays showed no significant differences in liver and renal function parameters between CK-treated groups and the normal group. Hemogram analysis indicated that CK did not lead to a decrease in immune cell levels in peripheral blood across all groups, suggesting no immune impairment by CK. Our animal experiment results indicated that mice treated with CK maintained higher body weights compared to those treated with cisplatin, indicating the lack of toxic effects from CK. Additionally, we explored the potential underlying mechanism of CK's anti-cancer effect on SCLC, revealing its association with inducing cell cycle arrest and apoptosis.

A number of research studies have highlighted that certain anti-cancer agents trigger the cell cycle arrest checkpoint, consequently promoting apoptotic cell demise. Notably, the unregulated cell cycle stands as a characteristic trait of cancer cells, playing a significant role in cancer advancement and progression.^[34,35] Cdks, controlled by interactions with cyclins specific to the cell cycle and Cdk inhibitors, are the primary regulators of the central machines that drive cell cycle progress. Cdk4 and Cdk6 form a complex with cyclin D during the G1 to S phase. The cyclin B/CDK1 complex induces the G2/M transition and processes during mitosis, while cyclin A/Cdc2 and Cdk2 complex regulate the S and G2 phases.^[36] P53 and P21 protein levels increase in

response to DNA damage, controlling the CDK2-cyclin E complex downstream.^[37]

Apoptosis is a kind of genetically programmed cell death that is tightly regulated and frequently studied in human lung cancer. Numerous cancer cells have been shown to undergo apoptosis when exposed to the ginsenosides Rk1 and Rk3.^[38,39] Our findings demonstrated that CK triggered apoptotic cell death, a conclusion supported by AO/EB and Annexin V-FITC/PI double staining. The Bcl-2 protein family, pivotal in the intrinsic mitochondrial apoptosis pathway, plays a vital role in programmed cell death. This pathway is activated in response to cellular damage or when a cell is deemed unnecessary, involving the release of cytochrome c from the mitochondria, initiating a cascade of events culminating in cell death. Pro-apoptotic proteins like Bax and Bak act as gatekeepers to the mitochondrial apoptosis pathway, their activation marked by multiple conformational changes and intramembranous homo-oligomerization within the mitochondria. The Bcl-2 family of proteins governs the intrinsic apoptosis pathway, essential for proper cell cycle functioning. The disrupted regulation of the cell cycle is a characteristic feature of cancer, resulting from a breakdown in the mechanisms overseeing the cell cycle and leading to uncontrolled cell division.^[40] Bax modifies the permeability of the mitochondrial membrane, causing the release of cytochrome-c from the space between mitochondrial membranes into the cytoplasm. This event triggers the activation of caspase-9, subsequently leading to the activation of caspase-3. Ultimately, these cascading processes culminate in the cleavage of PARP proteins and the initiation of the intrinsic apoptosis pathway.^[41] In this study, the evaluation of caspase activities, JC-10, and western blot assays collectively illustrated that CK induced apoptosis in lung cancer cells through the caspase-dependent intrinsic signaling pathway. These findings are consistent with prior research on apoptosis mechanisms in cancer. Specifically, our investigation disclosed that CK prompted apoptosis in small-cell lung cancer (SCLC) cells by activating Bax, cleaved caspase-3, cleaved caspase-9, and PARP, while simultaneously reducing the protein levels of Bcl-2. This implies that CK initiates apoptosis by triggering the intrinsic mitochondrial pathway within SCLC cells. Upon activation, p53 assumes a pivotal role in coordinating a halt in the cell cycle, facilitating DNA repair or apoptosis to counteract the proliferation of cells with substantial DNA damage. This is achieved through the transactivation of genes associated with initiating cell cycle arrest and/or apoptosis.^[42]

Studies have shown that genistein, a compound found in soybeans, induces cell cycle arrest at the G2/M phase through the p53/ATM pathway in a dependent manner.

Once induced, p53 acts as a transcription factor, regulating various genes involved in apoptosis, senescence, and cell cycle arrest. In the early stages of tumor development, genomic instability and DNA damage lead to p53 activation, which mediates tumor suppression. DNA damage response (DDR) is the response of cells to genotoxic pressure, including DNA repair, cell cycle arrest (cell cycle arrest), and apoptosis.^[43] The genetic material of eukaryotic cells can be replicated correctly and passed on to the next generation mainly because the cells have a set of effective DNA damage response mechanisms. Ataxia-telangiectasia-mutated ATM and Rad-3 related proteins (ATM and Rad-3-related ATR) kinase can sense DNA damage and transduce DNA damage signal to downstream target protein activate stress system produces cell cycle arrest to complete DNA repair reactivate or initiate the apoptosis process.^[44] Therefore, ATM and ATR are very important to maintain the cell genome's stability and prevent tumors' occurrence. Chk1 and Chk2 are important substrates for ATM and ATR, and ATM/ATR after DNA damage allows Chk1 and Chk2 to obtain kinase activity Chk1 and Chk2 are activated, phosphorylating downstream Cdc25 family members and other substrates, transmitting damage signals downstream, and ultimately preventing the progression of the cell cycle. Both Chk1 and Chk2 kinases are silk/threonine protein kinases with certain substrate specificity and have different activation conditions. The ATR signaling pathway downregulates cyclin protein B1 expression to stop cell mitosis for the detection and repair of DNA damage.^[45] In this study, we uncovered the potent anti-tumor effects of ginsenoside CK on small cell lung cancer (SCLC) through both apoptosis and cell cycle arrest pathways. The efficacy of ginsenoside CK against cancer displayed a dose-dependent correlation, and CK initiated a robust DNA damage response, as indicated by increased phosphorylation of CDC25C, CDK1, ATM/ATR, and CHK2/CHK1, leading to G2/M cell cycle arrest. Treatment with ginsenoside CK led to a reduction in tumor burden without eliciting adverse effects on hematologic or hepatorenal functions in the animal model. Moreover, the expression of γ -H2AX increased in proportion to the rising CK concentration, signifying the activation of the DNA damage response (DDR). Subsequent phosphorylation of ATM, ATR, CHK2, and CHK1 impeded the CDK1–cyclin B1 complex by deactivating CDC25C, impeding G2/M transition and inducing cell cycle arrest. This G2/M arrest heightened the susceptibility of tumor cells to radiation, thereby amplifying the overall anti-tumor efficacy of ginsenoside CK. Through the upregulation of ATM/ATR/CHK2/CHK1 signaling pathways, ginsenoside CK demonstrated its capacity to impede cell proliferation, induce apoptosis, and prompt cell cycle arrest in H1688 and DMS114 SCLC cells.

Conclusion

In summary, our experimental results represent the first evidence that ginsenoside CK effectively inhibits cell proliferation, induces apoptosis, and causes cell cycle arrest at the G2/M phase by activating the ATM/ATR pathway in small-cell lung cancer. Moreover, ginsenoside CK demonstrated the ability to suppress the growth of SCLC xenograft tumors without adversely affecting normal bronchial epithelium viability, as well as maintaining the integrity of hematological and hepatorenal functions. These findings suggest that CK holds promise as a novel therapeutic agent for the future treatment of human SCLC.

Disclosures

Ethics Committee Approval: Approval of the research protocol by an Institutional Reviewer Board.

Animal Studies: The experimental protocol involving animals received approval from the Animal Ethics Committee of Northwest University (NWU-AWC-20210304M).

Peer-review: Externally peer-reviewed.

Conflict of Interest: None declared.

Funding Information: This work was financially supported by the National Key R&D Program of China (2021YFC2101500), the National Natural Science Foundation of China (22078264 and 22108223), the Key R&D Program of Shaanxi (2022ZDLSF05-12), Natural Science Foundation of Shaanxi (2019JQ-259), Xian Association for Science and Technology Youth Talent Support Plan (095920211301), and the Xi'an Science and Technology Project (20191422315KYPT014JC016 and 20GXSF0004).

Authorship Contributions: Conceptualization: P.F., J.Z., L.Q.; Methodology: P.F., J.Z., L.Q.; Software: P.F., J.Z., L.Q.; Validation: P.F., J.Z., L.Q.; Formal Analysis: P.F., J.Z., L.Q.; Investigation: P.F., J.Z., L.Q., D.F.; Resources: R.H., D.F., X.M.; Data Curation: P.F., J.Z., L.Q., D.F.; Writing—Original Draft Preparation: P.F., J.Z., L.Q.; Writing—Review and Editing: P.F., J.H., L.Q.; Visualization: P.F., J.Z., L.Q.; Supervision: D.F.; Project Administration: X.M., R.H., D.F.; Funding Acquisition: X.M., R.H., D.F.

References

1. Aggarwal A, Lewison G, Idir S, Peters M, Aldige C, Boerckel W, et al. The state of lung cancer research: A global analysis. *J Thorac Oncol* 2016;11:1040–50.
2. Van Meerbeeck JP, Fennell DA, De Ruyscher DKM. Small-cell lung cancer. *Lancet* 2011;378:1741–55.
3. Guo W, Qiao T, Li T. The role of stem cells in small-cell lung cancer: Evidence from chemoresistance to immunotherapy. *Semin Cancer Biol* 2022;87:160–169.
4. Chang JS, Chen LT, Shan YS, Lin SF, Hsiao SY, Tsai CR, et al. Comprehensive analysis of the incidence and survival patterns of lung cancer by histologies, including rare subtypes, in the era of molecular medicine and targeted therapy: A nation-wide

- cancer registry-based study from Taiwan. *Medicine* Baltimore 2015;94:e969.
5. Oze I, Hotta K, Kiura K, Ochi N, Takigawa N, Fujiwara Y, et al. Twenty-seven years of phase III trials for patients with extensive disease small-cell lung cancer: Disappointing results. *PLoS One* 2009;4:e7835.
 6. Bi N, Cao J, Song Y, Shen J, Liu W, Fan J, et al. A microRNA signature predicts survival in early stage small-cell lung cancer treated with surgery and adjuvant chemotherapy. *PLoS One* 2014;9:e91388.
 7. Fang C, Zhang J, Qi D, Fan X, Luo J, Liu L, et al. Evodiamine induces G2/M arrest and apoptosis via mitochondrial and endoplasmic reticulum pathways in H446 and H1688 human small-cell lung cancer cells. *PLoS One* 2014;9:e115204.
 8. Joshi M, Ayoola A, Belani CP. Small-cell lung cancer: An update on targeted therapies. *Impact Genet Targets Cancer Ther* 2013;385–404.
 9. Hann CL, Rudin CM. Management of small-cell lung cancer: Incremental changes but hope for the future. *Oncol Williston Park* 2008;22:1486.
 10. Dai L, Smith CD, Foroozesh M, Miele L, Qin Z. The sphingosine kinase 2 inhibitor ABC294640 displays anti-non-small cell lung cancer activities in vitro and in vivo. *Int J Cancer* 2018;142:2153–62.
 11. Chan BA, Coward JIG. Chemotherapy advances in small-cell lung cancer. *J Thorac Dis* 2013;5:S565.
 12. Huang MY, Zhang LL, Ding J, Lu JJ. Anticancer drug discovery from Chinese medicinal herbs. *Chin Med* 2018;13:1–9.
 13. Yue PY, Mak NK, Cheng YK, Leung KW, Ng TB, Fan DT, et al. Pharmacogenomics and the Yin/Yang actions of ginseng: Anti-tumor, angiomodulating and steroid-like activities of ginsenosides. *Chin Med* 2007;2:1–21.
 14. Li C, Dong Y, Wang L, Xu G, Yang Q, Tang X, et al. Ginsenoside metabolite compound K induces apoptosis and autophagy in non-small cell lung cancer cells via AMPK–mTOR and JNK pathways. *Biochem Cell Biol* 2019;97:406–14.
 15. Zhang S, Zhang M, Chen J, Zhao J, Su J, Zhang X. Ginsenoside compound K regulates HIF-1 α -mediated glycolysis through bclaf1 to inhibit the proliferation of human liver cancer cells. *Front Pharmacol* 2020;11:583334.
 16. Zhou L, Li Z, Li C, Liang Y, Yang F. Anticancer properties and pharmaceutical applications of ginsenoside compound K: A review. *Chem Biol Drug Des* 2022;99:286–300.
 17. Liu J, Wang Y, Yu Z, Lv G, Huang X, Lin H, et al. Functional mechanism of ginsenoside compound K on tumor growth and metastasis. *Integr Cancer Ther* 2022;21:15347354221101204.
 18. Bakkenist CJ, Kastan MB. Initiating cellular stress responses. *Cell* 2004;118:9–17.
 19. Abraham RT. Cell cycle checkpoint signaling through the ATM and ATR kinases. *Genes Dev* 2001;15:2177–96.
 20. Appella E, Anderson CW. Post-translational modifications and activation of p53 by genotoxic stresses. *Eur J Biochem* 2001;268:2764–72.
 21. Chen Y, Poon RYC. The multiple checkpoint functions of CHK1 and CHK2 in maintenance of genome stability. *Front Biosci* 2008;13:5016–29.
 22. Liu Q, Guntuku S, Cui XS, Matsuoka S, Cortez D, Tamai K, et al. Chk1 is an essential kinase that is regulated by Atr and required for the G2/M DNA damage checkpoint. *Genes Dev* 2000;14:1448–59.
 23. Zhang B, Fu R, Duan Z, Shen S, Zhu C, Fan D. Ginsenoside CK induces apoptosis in triple-negative breast cancer cells by targeting glutamine metabolism. *Biochem Pharmacol* 2022;202:115101.
 24. Lowe SW, Ruley HE, Jacks T, Housman DE. p53-Dependent apoptosis modulates the cytotoxicity of anticancer agents. *Cell* 1993;74:957–67.
 25. Banin S, Moyal L, Shieh SY, Taya Y, Anderson CW, Chessa L, et al. Enhanced phosphorylation of p53 by ATM in response to DNA damage. *Science* 1998;281:1674–7.
 26. Hirao A, Kong YY, Matsuoka S, Wakeham A, Ruland J, Yoshida H, et al. DNA damage-induced activation of p53 by the checkpoint kinase Chk2. *Science* 2000;287:1824–7.
 27. Canman CE, Lim DS, Cimprich KA, Taya Y, Tamai K, Sakaguchi K, et al. Activation of the ATM kinase by ionizing radiation and phosphorylation of p53. *Science* 1998;281:1677–9.
 28. Smith J, Tho LM, Xu N, Gillespie DA. The ATM–Chk2 and ATR–Chk1 pathways in DNA damage signaling and cancer. *Adv Cancer Res* 2010;108:73–112.
 29. Böttger F, Semenova EA, Song JY, Ferone G, van der Vliet J, Cozijnsen M, et al. Tumor heterogeneity underlies differential cisplatin sensitivity in mouse models of small-cell lung cancer. *Cell Rep* 2019;27:3345–58.
 30. Sarvi S, Mackinnon AC, Avlonitis N, Bradley M, Rintoul RC, Rassl DM, et al. CD133+ cancer stem-like cells in small cell lung cancer are highly tumorigenic and chemoresistant but sensitive to a novel neuropeptide antagonist. *Cancer Res* 2014;74:1554–65.
 31. Chen H, Wu L, Li X, Zhu Y, Wang W, Xu C, et al. Ginsenoside compound K inhibits growth of lung cancer cells via HIF-1 α -mediated glucose metabolism. *Cell Mol Biol* 2019;65:48–52.
 32. Chen L, Meng Y, Sun Q, Zhang Z, Guo X, Sheng X, et al. Ginsenoside compound K sensitizes human colon cancer cells to TRAIL-induced apoptosis via autophagy-dependent and -independent DR5 upregulation. *Cell Death Dis* 2016;7:e2334.
 33. Hu C, Song G, Zhang B, Liu Z, Chen R, Zhang H, et al. Intestinal metabolite compound K of panaxoside inhibits the growth of gastric carcinoma by augmenting apoptosis via Bid-mediated mitochondrial pathway. *J Cell Mol Med* 2012;16:96–106.
 34. Zheng WL, Wang BJ, Wang L, Shan YP, Zou H, Song RL, et al. ROS-mediated cell cycle arrest and apoptosis induced by zearalenone in mouse sertoli cells via ER stress and the ATP/

- AMPK pathway. *Toxins Basel* 2018;10:24.
35. Chong D, Ma L, Liu F, Zhang Z, Zhao S, Huo Q, et al. Synergistic antitumor effect of 3-bromopyruvate and 5-fluorouracil against human colorectal cancer through cell cycle arrest and induction of apoptosis. *Anticancer Drugs* 2017;28:831–40.
36. Sanchez-Martinez C, Gelbert LM, Lallena MJ, de Dios A. Cyclin dependent kinase (CDK) inhibitors as anticancer drugs. *Bioorg Med Chem Lett* 2015;25:3420–35.
37. Li Y, Jenkins CW, Nichols MA, Xiong Y. Cell cycle expression and p53 regulation of the cyclin-dependent kinase inhibitor p21. *Oncogene* 1994;9:2261–8.
38. Kim YJ, Kwon HC, Ko H, Park JH, Kim HY, Yoo JH, et al. Anti-tumor activity of the ginsenoside Rk1 in human hepatocellular carcinoma cells through inhibition of telomerase activity and induction of apoptosis. *Biol Pharm Bull* 2008;31:826–30.
39. Duan Z, Deng J, Dong Y, Zhu C, Li W, Fan D. Anticancer effects of ginsenoside Rk3 on non-small cell lung cancer cells: In vitro and in vivo. *Food Funct* 2017;8:3723–36.
40. Ola MS, Nawaz M, Ahsan H. Role of Bcl-2 family proteins and caspases in the regulation of apoptosis. *Mol Cell Biochem* 2011;351:41–58.
41. Liang L, He T, Du T, Fan Y, Chen D, Wang Y. Ginsenoside Rg5 induces apoptosis and DNA damage in human cervical cancer cells. *Mol Med Rep* 2015;11:940–6.
42. Ozaki T, Nakagawara A. Role of p53 in cell death and human cancers. *Cancers Basel* 2011;3:994–1013.
43. Ljungman M. The DNA damage response—repair or despair? *Environ Mol Mutagen* 2010;51:879–93.
44. Yang J, Yu Y, Hamrick HE, Duerksen-Hughes PJ. ATM, ATR and DNA-PK: Initiators of the cellular genotoxic stress responses. *Carcinogenesis* 2003;24:1571–80.
45. Liu K, Zheng M, Lu R, Du J, Zhao Q, Li Z, et al. The role of CDC25C in cell cycle regulation and clinical cancer therapy: A systematic review. *Cancer Cell Int* 2020;20:1–16.